A Truncated Progesterone Receptor (PR-M) Localizes to the Mitochondrion and Controls Cellular Respiration

Qunsheng Dai, Anish A. Shah, Rachana V. Garde, Bryan A. Yonish, Li Zhang, Neil A. Medvitz, Sara E. Miller, Elizabeth L. Hansen, Carrie N. Dunn, and Thomas M. Price

Departments of Obstetrics and Gynecology (Q.D., A.A.S., R.V.G., B.A.Y., E.L.H., C.N.D., T.M.P.) and Pathology (N.A.M., S.E.M.), Duke University, Durham, North Carolina 27710; and Shenzhen Maternal and Child Healthcare Hospital (L.Z.), Shenzhen, Guangdong Province 518045, China

The cDNA for a novel truncated progesterone receptor (PR-M) was previously cloned from human adipose and aortic cDNA libraries. The predicted protein sequence contains 16 unique N-terminal amino acids, encoded by a sequence in the distal third intron of the progesterone receptor *PR* gene, followed by the same amino acid sequence encoded by exons 4 through 8 of the nuclear *PR*. Thus, PR-M lacks the N terminus A/B domains and the C domain for DNA binding, whereas containing the hinge and hormone-binding domains. In this report, we have localized PR-M to mitochondria using immunofluorescent localization of a PR-M-green fluorescent protein (GFP) fusion protein and in Western blot analyses of purified human heart mitochondrial protein. Removal of the putative N-terminal mitochondrial localization signal obviated association of PR-M with mitochondria, whereas addition of the mitochondrial localization signal to green fluorescent protein resulted in mitochondrial localization. Immunoelectron microscopy and Western blot analysis after mitochondrial fractionation identified PR-M in the outer mitochondrial membrane. Antibody specificity was shown by mass spectrometry identification of a PR peptide in a mitochondrial membrane protein isolation. Cell models of overexpression and gene silencing of PR-M demonstrated a progestin-induced increase in mitochondrial membrane potential and an increase in oxygen consumption consistent with an increase in cellular respiration. This is the first example of a truncated steroid receptor, lacking a DNA-binding domain that localizes to the mitochondrion and initiates direct non-nuclear progesterone action. We hypothesize that progesterone may directly affect cellular energy production to meet the increased metabolic demands of pregnancy. **(*Molecular Endocrinology* 27: 741–753, 2013)**

Progesterone is a reproductive hormone, because elevated circulating levels are found in women only during the luteal phase of the reproductive cycle and during pregnancy. Classically, responses to progesterone are mediated in target tissues by 2 isoforms of the nuclear receptors, progesterone receptor (PR)-A and PR-B (1). The structure of nuclear PRs (nPRs) include an N-terminal A/B domain that regulates transcriptional efficiency, the C domain or DNA-binding domain (DBD), the D domain or hinge region, and the E/F domains responsible for hormone binding (hormone-binding domain [HBD]) (2).

Progesterone is known to regulate transcription. However, other responses to progesterone occur that are too rapid to be mediated only through transcriptional regulation or take place in cells that are believed to lack classical nPRs. Several candidate receptors responsible for these actions have been investigated. A *Xenopus* PR (XPR) has significant homology to the human PR in the

ISSN Print 0888-8809 ISSN Online 1944-9917
Printed in U.S.A.

Received August 28, 2012. Accepted March 18, 2013.
First Published Online March 21, 2013

Abbreviations: DBD, DNA-binding domain; ER, estrogen receptor; GFP, green fluorescent protein; GR, glucocorticoid receptor; HBD, hormone-binding domain; HSD, honestly significant difference; ψm, mitochondrial membrane potential; MLS, mitochondrial localization signal; MPA, medroxyprogesterone acetate; MR, metabolic rate; nPR, nuclear PR; PR, progesterone receptor; RNAi, RNA interference; SDS, sodium dodecyl sulfate; siRNA, small interfering RNA; TMRM, tetramethylrhodamine methyl ester; UTR, untranslated region.

DBD and the HBD but poor sequence similarity in the remainder of the protein (3). In other cases, proteins with no sequence similarity to the nPR have been identified. A G protein-coupled membrane receptor with 3 isotypes showing high specific progestin binding was characterized from spotted seatrout ovaries (MPRα, -β, and -γ) (4). Another protein, named PR membrane component-1 (PGRMC1) has been identified by high-affinity progesterone binding in porcine liver microsomes (5), and the corresponding cDNA was identified in a human liver cDNA library (6).

In contrast, nPRs may be responsible for nontranscriptional actions via interaction with cytosolic proteins. A direct interaction between a polyproline motif in the N-terminal domain of the classic nPR and the SRC homology 3 domain of c-Src has been shown in molecular studies (7, 8).

This report focuses on a 38-kDa truncated PR, named PR-M, of which the cDNA was originally cloned from human adipose and aortic cDNA libraries (AY212933) (9). Expression of PR-M was demonstrated by Western blot analysis in T47D breast cancer cells, in T47D-Y breast cancer cells lacking expression of nPR (10), and in human aortic endothelial cells (9). Here, we report localization of PR-M to the mitochondrion. Progestin action via PR-M was demonstrated by an increase in mitochondrial membrane potential (ψm) with a corresponding increase in oxygen consumption, consistent with increased cellular respiration. Progesterone action via PR-M may be a key mechanism for meeting the increased metabolic demands of pregnancy.

Materials and Methods

See also Supplemental Methods (published on The Endocrine Society's Journals Online web site at http://mend.endojournals.org).

Northern blot analysis

Poly-A RNA was isolated and underwent electrophoresis in a 1% formaldehyde gel and transferred to a nylon membrane (Nytran; VWR, West Chester, Pennsylvania) by upward capillary transfer. The membrane was hybridized overnight with a 5′ end-labeled [^{32}P]dATP *PR-M* oligonucleotide probe. The membrane was then stripped and reprobed for actin transcript in a similar fashion with a random primer labeled with [^{32}P]dCTP PCR-generated partial cDNA probe.

r6xHIS-PR-M generation

A partial cDNA for *PR-M* was generated by RT-PCR using total RNA isolated from T47D breast cancer cells. Protein expression was performed with the Expressway Cell-free *Escherichia coli* Expression System (Invitrogen, Carlsbad, California)] with the addition of 0.1% Triton X-100. HIS-tagged PR-M was purified with the ProBond Purification System (Life Technologies/Invitrogen) using denatured conditions with urea. The final protein product was characterized by 6 histidines on the N terminus, the complete amino acid sequence of PR-M, and an additional 35 amino acids on the carboxy terminus yielding a calculated size of 44 kDa.

PR-M/EGFP-N1, PR-M(−16aa)/EGFP-N1, +30aaEGFP/N1 constructs and transient transfection

Construction of plasmids expressing PR-M-green fluorescent protein (GFP) and GFP only has been previously reported (9, 11). PR-M-GFP contains 28 amino acids between the last amino acid of PR-M and the initial methionine of GFP. PR-M(−16aa)/EGFP-N1 encodes a fusion protein lacking the initial 16 amino acids of PR-M, referred to as PR-M(−16aa)-GFP. The pEGFP-N1 vector was used to generate a new construct named p+30aaEGFP-N1. p+30aaEGFP-N1 encodes a protein with the initial 30 amino acids of PR-M as the N terminus of GFP. Transient transfection was performed with a mixture of Fugene 6 transfection (Roche, Indianapolis, Indiana) or Lipofectamine (Life Technologies/Invitrogen, Grand island, New York).

Immunofluorescent antibody staining

Myometrial tissue and cells were fixed in paraformaldehyde and permeabilized with Triton X-100. Samples were reacted with a monoclonal antibody to mitochondrial porin and various anti-PR antibodies. Slides were observed with a Zeiss Axio Observer wide-field inverted fluorescence microscope and a Zeiss LSM 510 confocal microscope, ×40 to ×100 objective. When using the Zeiss LSM 510 confocal, 405 diode deep blue spectral line 488, argon laser spectral line 488, and 561 diode spectral line 561 were used.

Immunoelectron microscopy

Myometrial tissue was obtained from a deidentified female undergoing cesarean delivery and from a second premenopausal female undergoing hysterectomy. Reactions were performed with the rabbit C19 and mouse MAB 462 directed to the HBD and the mouse 6A1 directed to the N terminus of nPR. Techniques are further described in the Supplemental Methods. For the C19 antibody, pre-embedding immunolabeling was performed by cutting myometrium with a tissue slicer to 200-μm sections and incubating them with blockers, primary antibody followed by goat antirabbit conjugated to 0.08-nm gold particles. The gold size was enlarged with a silver solution. The tissue was dehydrated and embedded in epoxy resin and baked. Ultrathin sections were cut and stained with uranium and lead and then viewed in an electron microscope.

Western blot analysis

Purified human heart mitochondrial protein (Mitosciences, Eugene, Oregon) was separated by electrophoresis on a 10% Ready Tris-HCl gel (Bio-Rad Laboratories, Hercules, California) and was transferred to a polyvinylidene difluoride membrane. Commercial anti-PR antibodies included C19, MAB 462, AB 52, and 6A1. Antibodies used as cell fraction markers included prohibitin for mitochondria, histone deacetylase 1 for nucleus, syntaxin 6 for endoplasmic reticulum, mitochondrial porin for mitochondrial outer membrane, and complex III subunit core 1 for mitochondrial inner membrane.

Mass spectrometry

In-gel tryptic digestions were performed as previously described (12). Peptides were then extracted with acetonitrile. Samples were analyzed (25 fmol of ADH as internal standard) using a nanoAcquity UltraPerformance Liquid Chromatography system coupled to a Synapt G2 mass spectrometer (Waters Corporation, Milford, Massachusetts). Peptide/protein identifications were made with Mascot version 2.2 (Matrix Science). Peptide and protein identifications were validated using PeptideProphet and ProteinProphet algorithm as deployed in Scaffold version 3.3.1. The Scaffold file containing tandem mass spectrometry data spectra, and associated search results have been made publicly available at https://discovery.genome.duke.edu/express/resources/2124/PRM_Price_030212.sf3.

Isolation of mitochondria from human myometrium tissue

Mitochondria were isolated through a sucrose gradient with ultracentrifugation as previously described with minor modifications (13).

Prefractionation of myometrial mitochondria and immunoprecipitation

Prefractionation of membrane protein was performed by detergent-based aqueous 2-phase system using 5% Triton X-114 as described (14). Isolated human myometrium mitochondrial membrane proteins were immunoprecipitated using MAB 462 antibody with a Pierce Crosslink IP kit (Thermo Scientific, Waltham, Massachusetts) according to the manufacturer's protocol. The eluted protein was boiled in sodium dodecyl sulfate (SDS)-sample buffer and subjected to 10% SDS-PAGE gel.

Human heart mitochondrial subfractionation

Mitochondrial inner and outer membrane fractions were prepared from human heart muscle using digitonin (Sigma Chemical, St. Louis, MO) based on previously published methods with minor modifications described in the Supplemental methods (15).

Tet-On expression

The complete coding sequence of *PR-M* was PCR generated from the PR-M/EGFP-N1 plasmid with a Kozak sequence and ligated into the pTRE-TIGHT vector (Clontech, Palo Alto, California). HeLa cells expressing the reverse tetracycline-controlled transactivator (rtTA) were transfected with pTRE-PR-M plasmid. PR-M expression was induced with 500 ng/mL doxycycline.

RNA interference transfection

T47D cells were transfected with 4 customized small interfering RNA (siRNA) duplexes directed to exons 1, 2, and 4 of *PR-M* (Thermo Scientific/Dharmacon) diluted in OPTI-MEM (Life Technologies/Invitrogen) and transfected with Lipofectamine 2000 (Life Technologies/Invitrogen). For silencing of *nPR*, cells were similarly transfected with 2 customized siRNA duplexes (Life Technologies/Invitrogen) directed to exons 1 and 2 of *nPR*.

Semiquantitative RT-PCR and SYBR Green quantitative real-time RT-PCR

Deoxyribonuclease I-treated total RNA (1 μg) was used for first-strand cDNA synthesis with an oligo(deoxythymidine) primer. Semiquantitative PCR was performed for amplifying *PR-M*, *nPR A* and *B*, and glyceraldehyde-3-phosphate dehydrogenase (*GAPDH*) cDNA under the same PCR condition, 25–30 cycles each.

Quantitative real-time RT-PCR with SYBR Green was performed after first-strand cDNA synthesis as above. Melt-curve analysis was performed on each assay in addition to 3 negative controls including absence of RNA in first-strand synthesis, absence of cDNA, and absence of polymerase enzyme. Assays with abnormal controls were excluded as were reactions with abnormal melt curves. All products were verified by sequence analysis.

Mitochondrial membrane potential

The ψm was determined with 5,5′,6,6′-tetrachloro-1,1′,3,3′-tetraethylbenzimidazolecarbocyanide iodine (JC-1) dye (Life Technologies/Invitrogen) as previously described (16) or with 20nM tetramethylrhodamine methyl ester (TMRM) (17).

Cell respiration assay

HeLa Tet-on cells transfected with pTRE or pTRE-PR-M plasmid were treated with doxycycline for induction of PR-M. After 72 hours, cells were treated with progestin R5020 (10^{-8}M) or vehicle (alcohol). The change in extracellular oxygen over 30 minutes was determined with a fluorescent probe (Luxcel Biosciences, Cork, Ireland).

Statistical analysis

Statistical tests were performed at the 2-sided $\alpha = 0.05$ level. All statistical analyses were performed using PASW Statistics version 18. Relative mRNA levels after RNA interference (RNAi) were determined by quantitative real-time RT-PCR analyzed by the $\Delta\Delta$ cycle threshold method (18) using the untransfected cells as the reference. Mock control scrambled siRNA and targeted siRNA values were compared with univariate ANOVA with the Tukey honestly significant difference (HSD) method for post hoc testing. Data for ψm were analyzed with univariate ANOVA with the Scheffé method of post hoc testing when experimental group numbers varied between treatments or Tukey HSD method for post hoc testing when experimental group numbers were the same between treatments. Linear trend analysis was performed with 1-way ANOVA. Ψm assays were performed in multiwell plates. Figures show the number of experiments performed on different days and the total number of observations, reflecting the number of wells analyzed. Statistical analysis was performed based on the number of experiments performed on different days. Data from the cell respiration assay were analyzed with repeated-measures ANOVA by the Tukey HSD method for post hoc testing.

Results

Northern analysis shows 6.1- and 2.5-kb transcripts for PR-M

Review of the human genome sequence shows that the 5′ untranslated region (UTR) and coding sequence for the

first 16 amino acids of PR-M correspond to sequence in the distal third intron of the *PR* gene just before the fourth exon. The remaining coding sequence is identical to exons 4 through 8 of the *nPR* cDNA. Hydropathy analysis shows that the 16 initial amino acids are strongly hydrophobic, with multiple phenylalanines (Figure 1A and Supplemental Table 1). Compared with PR-B and -A, the predicted protein structure of PR-M lacks the N-terminal A/B regions, the DBD, and the nuclear localization signal found in the third exon (19) but contains the hinge region and HBD. Previously published Northern blot analyses of T47D breast cancer cells using partial cDNA probes, including C-terminal coding sequence, identified 6 to 9 bands. The predominant 6 bands include sizes of 2.5, 3.2, 4.5, 6.1, and 11.4 kb. The 11.4-kb band appears as a tetrad with bands denoted I to IV (20, 21). Figure 1B shows Northern blot analyses of poly-A RNA hybridized with a dATP end-labeled 43-bp oligonucleotide probe directed to the 5′ UTR of *PR-M*. We demonstrate transcripts encoding PR-M at 6.1 and 2.5 kb in T47D and MCF-7 breast cancer cells expressing nPR, T47D-Y and MDA-MB-231 breast cancer cells not expressing nPR, and MCF-10A breast epithelial cells not expressing nPR (10, 22–25). The transition start site has not yet been experimentally identified for PR-M; thus, we cannot determine which transcript encodes PR-M.

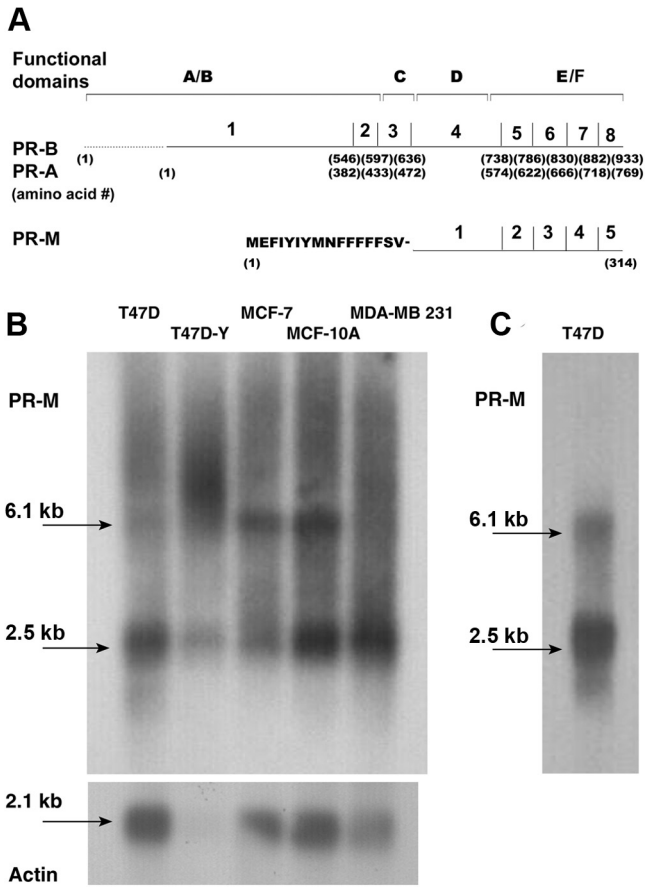

Figure 1. PR-M structure. A, Schematic diagram of the functional domains, exons, and amino acid number for nuclear PR-B, PR-A, and PR-M. B, Northern analysis of poly-A RNA from breast cancer and breast epithelial cell lines, hybridized with a 43-bp [^{32}P]ATP end-labeled probe directed to the 5′ UTR, shows predominant bands at 6.1 and 2.5 kb. C, A repeat, clearer, Northern blot for T47D cells is shown. See also Supplemental Table 1.

Mass spectrometry identification of a PR peptide in mitochondrial protein

It is not feasible to develop a specific antibody to the unique N terminus of PR-M due to high hydrophobicity and poor antigenicity. Thus, we used a technique of selective antibody staining with commercially available antibodies directed to the N terminus of nPR (6A1 and PgR 636) that should not recognize PR-M and antibodies directed to the HBD (MAB 462 and C19) that should recognize nPR and PR-M. Because the specificity of PR antibodies directed to the HBD has been questioned (26), we verified antibody binding on Western blot analysis with a recombinant protein and with protein isolated from mitochondria identified as PR by mass spectrometry. Figure 2A shows binding of C19 and MAB 462 antibody to a recombinant HIS-tagged PR-M with a mass of 44 kDa generated in a cell-free *E. coli* system. The protein was purified under denaturing conditions using urea with a nickel column. In the same Western blot, an endogenous band at 38 kDa, consistent with PR-M, is seen in protein from T47D-Y cells known to lack expression of nPR (10). Another Western blot shows the 44-kDa rPR-M compared with endogenous 38-kDa PR-M in T47D cells known to express nPR. Figure 2B shows a SYPRO Ruby-stained gel of rPR-M and mitochondrial membrane protein isolated from human myometrium (before immunoprecipitation) with subsequent immunoprecipitation using the MAB 462 antibody. The presumed PR-M at 38 kDa in the immunoprecipitation preparation was examined by mass spectrometry and confirmed by the finding of peptide VLLLLNTIPLEGLR, encoded by a sequence within the last 2 exons of PR-M. Western blot analysis of the immunoprecipitation preparation with the C19 antibody shows binding of the same 38-kDa band. Other proteins identified in the same band included myosin-11, mitochondrial inner membrane protein, mitochondrial aconitate hydratase, and Ig κ-chain C.

PR-M localizes to the mitochondrion

Figure 3A shows confocal images of transfected Cos-1 cells expressing PR-M-GFP (GFP on the carboxy end) or expressing GFP alone. Mitochondria were stained with MitoFluor Red 589 or Mitotracker Red CMXRos. PR-M-GFP localized to mitochondria, whereas GFP showed

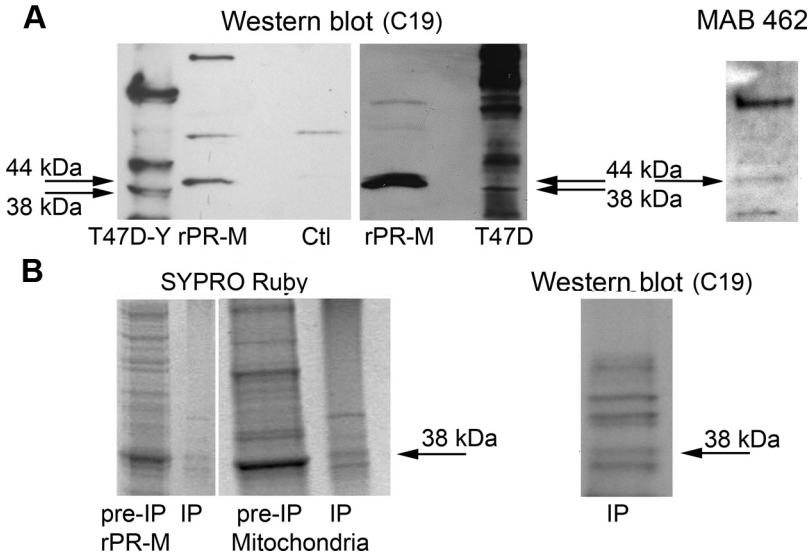

Figure 2. Identification of PR-M in mitochondria by mass spectrometry. A, Reaction with the C19 antibody in the left lane shows endogenous expression of a 38-kDa protein consistent with PR-M in T47D-Y breast cancer cells, known to lack expression of nPR. The next lane identifies a HIS-tagged rPR-M (44 kDa). rPR-M was generated in a cell-free *E. coli* system followed by a denaturing purification with urea on a nickel column. The control (Ctl) reaction lacked rPR-M template and showed no evidence of a band at 44 kDa. The right lane is from a different blot showing the 44-kDa rPR-M compared with the 38-kDa PR-M in T47D breast cancer cells. The far right blot shows the rPR-M also identified with the MAB 462 antibody. B, SYPRO Ruby-stained gel of rPR-M and mitochondrial membrane protein from human myometrial tissue before immunoprecipitation (pre-IP) and after immunoprecipitation (IP) with MAB 462 antibody, showing a similar protein banding pattern. The band at 38 kDa in the mitochondrial immunoprecipitation preparation submitted for mass spectrometry analysis showed a PR-specific peptide. Western blot analysis with the C19 antibody of the same mitochondrial immunoprecipitation preparation also identifies the 38-kDa protein.

diffuse intracellular distribution. Identical findings were seen with $HepG_2$ and HeLa/SF cells (Supplemental Figure 1, related to Figure 3). Cos-1 cells expressing a protein lacking the initial novel 16 amino acids (PR-M(-16aa)-GFP) showed no evidence of mitochondrial localization. Comparison of the N-terminus sequence of PR-M to known outer membrane mitochondrial proteins (Supplemental Table 1, related to Figure 1) showed similarity of the initial 30 amino acids, suggesting a mitochondrial localization signal (MLS). A GFP protein containing the initial 30 amino acids of PR-M on the N terminus (+30GFP) localized to the mitochondria. Previous studies of transfections with GFP-tagged nPR showed predominantly nuclear fluorescence (8, 27).

Further evidence of PR-M in the mitochondrion was gained with Western blot analysis of protein extracted from purified human heart mitochondria isolated by centrifugation through a Tris/sucrose buffer (28). Figure 3B shows Western blot analysis with C19 and MAB 462 anti-PR antibodies directed to the HBD. An intense band was seen at approximately 38 kDa consistent with PR-M. Less intense higher molecular weight bands of unclear origin were inconsistently seen with these 2 antibodies as shown in additional Western blots (Supplemental Figure 2, related to Figure 3). Significant contamination of the mitochondrial preparation with proteins from other organelles was analyzed using antibodies to the mitochondrial marker prohibitin, the endoplasmic reticulum marker syntaxin 6, and the nuclear marker histone deacetylase 1 (HDAC1) (Figure 3C). As expected, prohibitin was present in the mitochondrial preparation, whereas reactions with the other 2 antibodies were lacking. This suggests a lack of substantial contamination of the mitochondrial preparation with proteins from the endoplasmic reticulum or nucleus. The 38-kDa band was not seen with a monoclonal antibody (AB 52) directed to the N terminus of nPR (Figure 3D).

Selective immunohistochemical staining was used to investigate the presence of an endogenous mitochondrial PR in human myometrial tissue or cells after primary culture. The composite of immunofluorescent staining in Supplemental Figure 3 shows nuclear and non-nuclear staining with antibodies directed to the HBD, whereas only nuclear staining is seen with antibodies directed to the N terminus of nPR. A portion of the non-nuclear staining colocalized with mitochondrial staining.

We next identified PR-M predominantly on the outer membrane of the mitochondrion. Figure 4A shows a Western blot analysis after fractionation of purified heart mitochondria into fractions enriched with outer membrane and with mitoplasts (containing inner membrane and matrix proteins). The approximate 38-kDa protein consistent with PR-M was predominantly found in the outer membrane. Analyses performed for marker proteins showed appropriate enrichment of the fractions with voltage-dependent anion channel 1 (VDAC-1 or mitochondrial porin) used to identify the outer membrane and complex III subunit core I used to identify the mitoplast. A control blot with preabsorption of the MAB 462 antibody is shown in Supplemental Figure 4, related to Figure 4.

Immunoelectron microscopy of human myometrium was performed with the C19 and MAB 462 antibodies directed to the HBD and with the 6A1 antibody directed to the N terminus of nPR. Figure 4B shows images from reaction with the C19 antibody. Myocytes were seen with

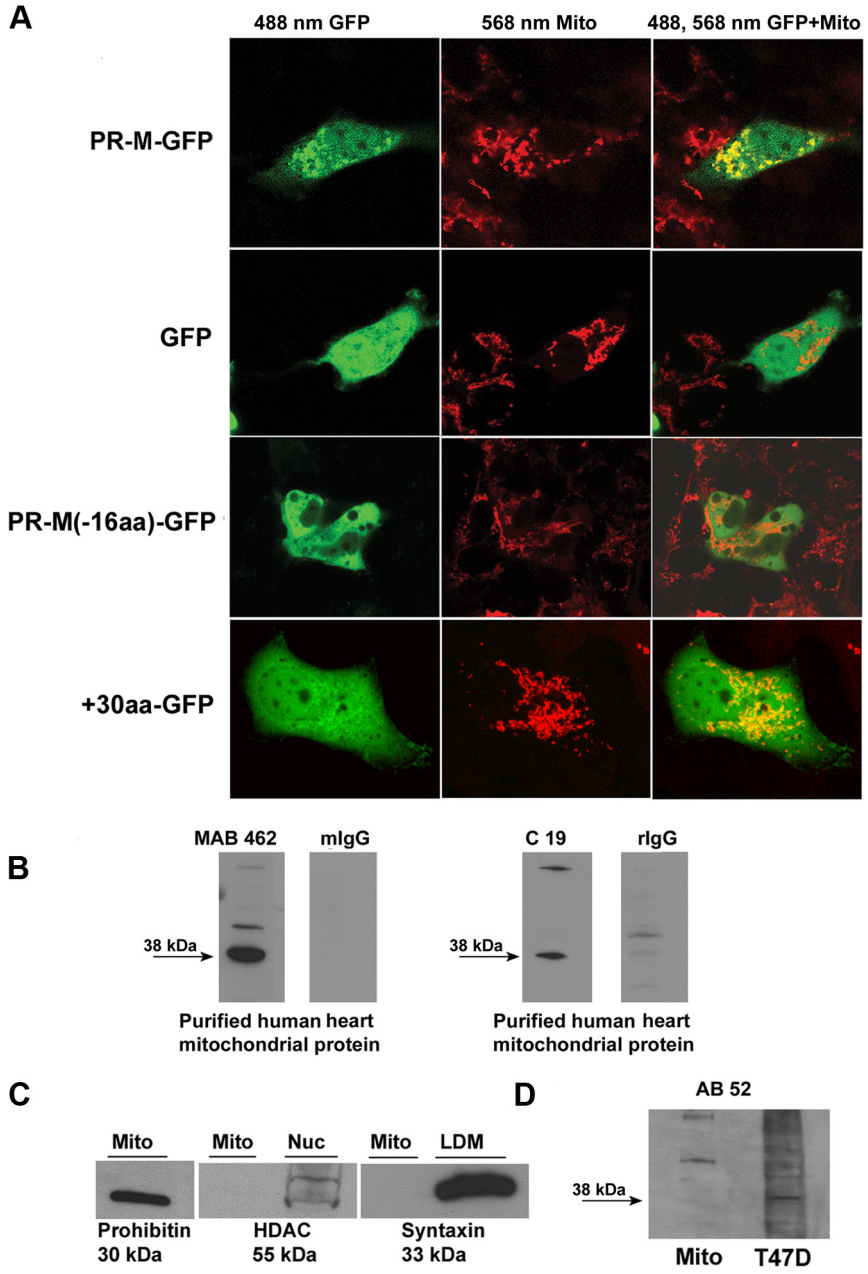

Figure 3. Mitochondrial localization of PR-M. A, Cos-1 cells transfected with a carboxy GFP-tagged PR-M (PR-M-GFP), control transfected GFP, a carboxy GFP-tagged truncated PR-M lacking the initial 16 amino acids (PR-M-16aa-GFP), or GFP containing the initial 30 amino acids of PR-M on the N terminus (+30-GFP). Mitochondria (Mito) are stained with Mitofluor or Mitotracker. Confocal imaging showed colocalization of stained mitochondria with PR-M-GFP and +30-GFP as shown by the yellow color. See also Supplemental Figure 1. B, Western blot analyses of purified human heart mitochondrial protein performed with a mouse antibody (MAB 462) and a rabbit antibody (C19) directed to the HBD of PR showed a predominant band at 38 kDa (PR-M). No specific binding was seen with replacement of the primary antibody with mouse or rabbit IgG. See also Supplemental Figure 2. C, Western blot analyses performed with antibodies to histone deacetylase (HDAC) and syntaxin 6 showed relative purity of the preparation. Prohibitin was used as a positive control. D, Western blot analysis with a mouse antibody (AB 52) directed to the N terminus of nPR showed no evidence of the 38-kDa PR-M protein. LDM, low density microsome.

(panel a) and without (panel b) nuclear staining, suggesting temporal expression of nPR. Non-nuclear staining was seen in all myocytes and predominantly involved the mitochondrial membrane, although some gold particles were seen in the cytosol. A minority of cells within the sample completely lacked staining (panel c). These cells appeared to have a different morphology and were likely not myocytes. A control reaction in which the antibody was preabsorbed with antigen (panel d) lacked nonspecific binding. Images of reactions with the MAB 462 and 6A1 antibodies are shown in Supplemental Figure 5. Similar to C19, reaction with MAB 462 showed nuclear and mitochondrial staining. In contrast, the 6A1 antibody directed to the N terminus of nPR only showed nuclear staining.

Progestin acting via PR-M increases ψm

Gene silencing in T47D breast cancer cells and inducible overexpression in Tet-On HeLa cells were used to investigate the role of PR-M in mitochondrial activity. Two RNAi assays were developed. In the first assay, 2 siRNA duplexes were designed to exons 1 and 2 of *nPR*, and in the second assay, 4 siRNA duplexes were designed to exons 1, 2, and 4 of *PR-M* corresponding to exons 4, 5, and 7 of *nPR*. Because PR-M is a truncated form of nPR, it is not feasible to design unique siRNA duplexes that recognize only *PR-M*. Silencing of *nPR* and *PR-M* transcripts were demonstrated by SYBR Green quantitative real-time RT-PCR (Figure 5, A and B) with melt curves shown in Supplemental Figure 6, related to Figure 5. A functional decrease in nPR activity was shown by inhibition of progestin-induced expression of the nuclear dot protein, *S100P* (Figure 5C) (29). The effect on ψm was determined by the change in fluorescent emission of JC-1. The fluorescent emission ratio (585/529) of JC-1 increases with mitochondrial membrane hyperpolarization, whereas the ratio decreases with mitochondrial membrane depolar-

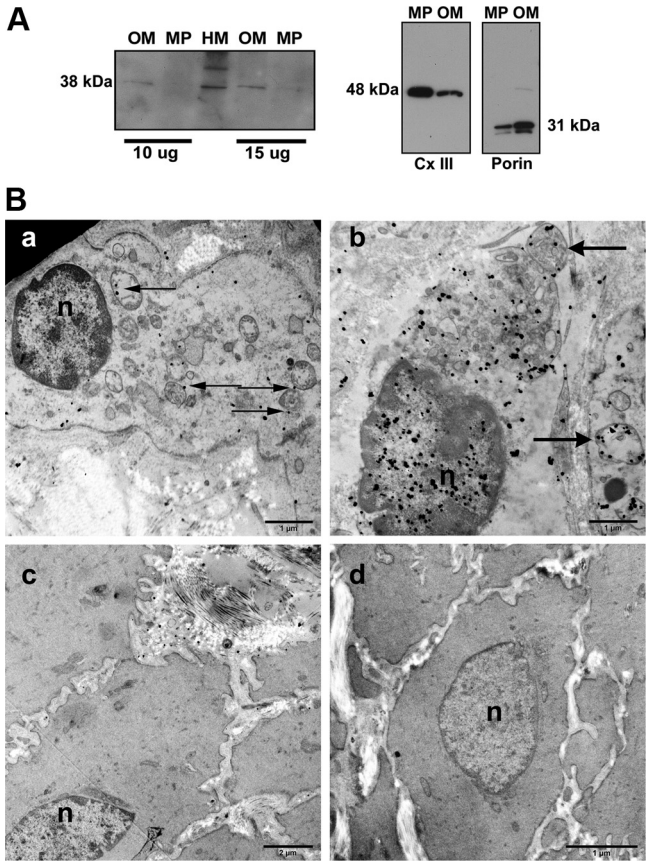

Figure 4. Localization of PR-M to the outer mitochondrial membrane. A, Western blot with MAB 462 of protein from human heart mitochondria (HM) and fractions enriched in proteins of the outer membrane (OM) and the inner membrane and matrix (mitoplast [MP]) showed the 38-kDa PR-M primarily in the OM. Enrichment of fractions was shown by reactions with antibodies to mitochondrial porin and to complex III subunit core I (Cx III), respectively. See also Supplemental Figures 3 and 4. B, Transmission electron microscopy of myometrial tissue with C19 antibody directed to the HBD. Note that the lack of tissue fixation in osmium (which would reduce or eliminate antigenicity) prevents the membranes from showing up as dark tracks. Panel a shows a myocyte without nuclear (n) staining. Mitochondrial staining predominantly of the outer membrane (arrows) is seen along with sparse cytosolic staining. Panel b shows a myocyte with nuclear staining and mitochondrial staining (arrows). Panel c shows a cell devoid of all staining. The morphology of this cell with sparse mitochondria suggests it is not a myocyte. Panel d shows a myocyte reacted with antigen-preabsorbed antibody lacking staining. Also see Supplemental Figure 5.

ization. Figure 5D shows that a progestin-induced increase in ψm is obviated by siRNA knockdown of PR-M in T47D cells. In contrast, there was no effect on progestin-induced increase in ψm with siRNA knockdown of nPR (Figure 5E).

In the second model, the complete coding sequence of PR-M was expressed in a Tet-On HeLa cell system. Figure 6A shows the results of a semiquantitative RT-PCR experiment demonstrating an increase in *PR-M* transcript levels after a 48-hour treatment with doxycycline. Figure 6B shows an increase in ψm with a 30-minute treatment with the progestin R5020 in transfected cells. No significant increase was seen in cells transfected with the control plasmid. ADP, used as a positive control, increases ψm by an increase in intracellular calcium via activation of a purinergic receptor (30). Figure 6C shows inhibition of the R5020-induced increase in ψm by the PR antagonist, RTI-6413-049b. Figure 6D shows results of a 60-minute treatment with medroxyprogesterone acetate (MPA) or progesterone compared with vehicle in Tet-On HeLa cells expressing PR-M and in control transfected cells. There was no statistically significant difference among the groups in either cell type. Analysis of the percent difference of MPA to ethanol vehicle and progesterone to ethanol vehicle did show a significant linear trend ($P = .038$ and $P = .05$, respectively) in cells expressing PR-M. No linear trend was seen in control transfected cells (Supplemental Figure 7, related to Figure 6) Interestingly, low levels of *PR-M* transcript were identified in untransfected and control plasmid transfected Tet-On HeLa cells, which historically lack detectable *nPR* transcripts (31) (Supplemental Figure 8, related to Figure 6). These cells did not appear to express adequate PR-M protein for a response to progestagens.

Reliability of the JC-1 indicator was corroborated by the use of TMRM. At low concentrations, this cationic dye is sequestered by active mitochondria with the red fluorescent emission correlating with ψm. As shown in Supplemental Figure 9, related to Figure 5, R5020 treatment of T47D cells increased TMRM emission compared with untreated and vehicle-treated cells. Control reactions showed increased ψm after treatment with oligomycin, which inhibits proton transport, increased ψm after addition of pyruvate, and decreased ψm after carbonyl cyanide 3-chlorophenylhydrazone treatment, which increases proton transport.

Progestin acting via PR-M increases cellular respiration

To demonstrate a progestin-mediated increase in cellular respiration, the change in extracellular oxygen level was measured. In a system closed to air, oxygen is depleted from the media during cellular respiration and can be measured with a cell-impermeable phosphorescent oxygen-sensitive probe (MitoXpress; Luxcel Biosciences). An increase in probe signal corresponds to depletion of extracellular oxygen. Figure 7A shows a kinetic experiment revealing an increase in oxygen consumption in Tet-On HeLa cells expressing PR-M treated with R5020. No increase was seen in vehicle-treated cells expressing PR-M or in cells transfected with the control vector. A difference in fluorescent emission was seen at time 0 (referring to the initiation of measurements) in cells express-

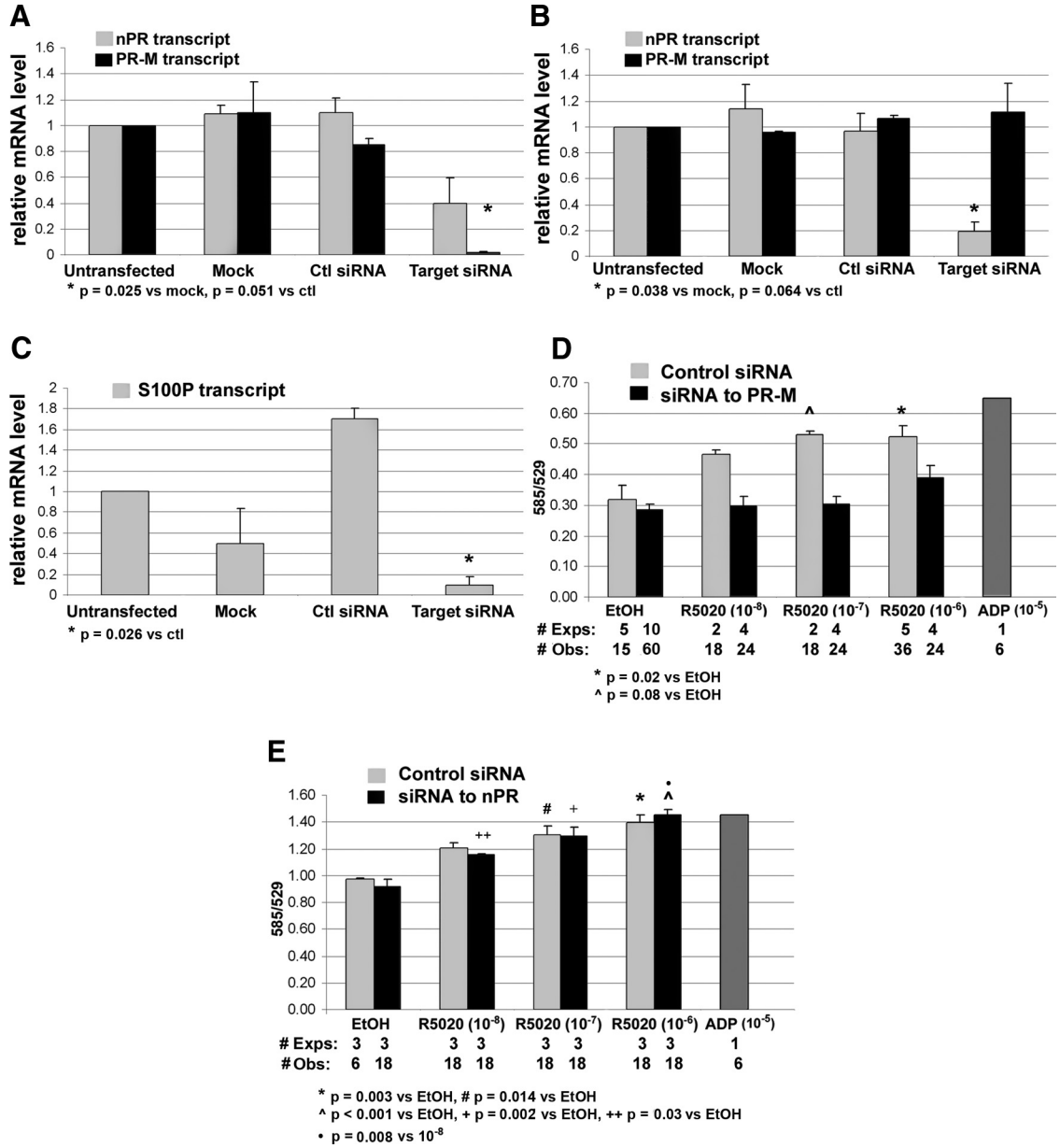

Figure 5. Change in ψm after RNAi in T47D breast cancer cells. A, Transfection with siRNA duplexes directed to exons 1, 2, and 4 of *PR-M* corresponding to exons 4, 5, and 7 of *nPR* decreased *PR-M* expression (dark bars), whereas a decrease in *nPR* transcript levels did not reach statistical significance (light bars, duplicate assays). B, Transfection with siRNA duplexes directed to exons 1 and 2 of *nPR* significantly decreased *nPR* expression (duplicate assays). C, Transfection with siRNA duplexes directed to exons 1 *and* 2 of nPR significantly decreased *S100P* transcript levels after 18 hours treatment with 10^{-8}M R5020 (duplicate assays). D, Transfection with siRNA to *PR-M* inhibited the increase in ψm with 30 minutes R5020 treatment (dark bars). Control siRNA transfected cells showed an increase in ψm (light bars). E, Transfection with siRNA to *nPR* showed an increase in ψm with 30 minutes R5020 treatment (dark bars), also seen with control siRNA transfected cells (light bars). ADP (10^{-5}M) served as a positive control. All values are expressed as mean ± SEM. See also Supplemental Figures 6 and 9. Abbreviations: Ctl, control; #Exps, number of experiments performed on different days; #Obs, total number of wells assayed.

ing PR-M treated with R5020 compared with vehicle. This difference was due to the time elapsed during placement of the samples into the plate and starting the reader. Figure 7B shows an absence of change in oxygen consumption when PR-M lacking the MLS (PR-M-30aa) was treated with R5020 or control. Positive controls for the assay included treatments with sodium pyruvate plus ADP, whereas treatment with rotenone served as a negative control.

Discussion

The predicted structure of PR-M is consistent with a mitochondrial protein (32). The novel N-terminal 16 amino acids are hydrophobic, characteristic of a transmembrane domain. Following this region are several positively charged hydrophilic amino acids. As shown in Supplemental Table 1, the initial 30 amino acids of PR-M are similar to N-terminally anchored outer membrane mito-

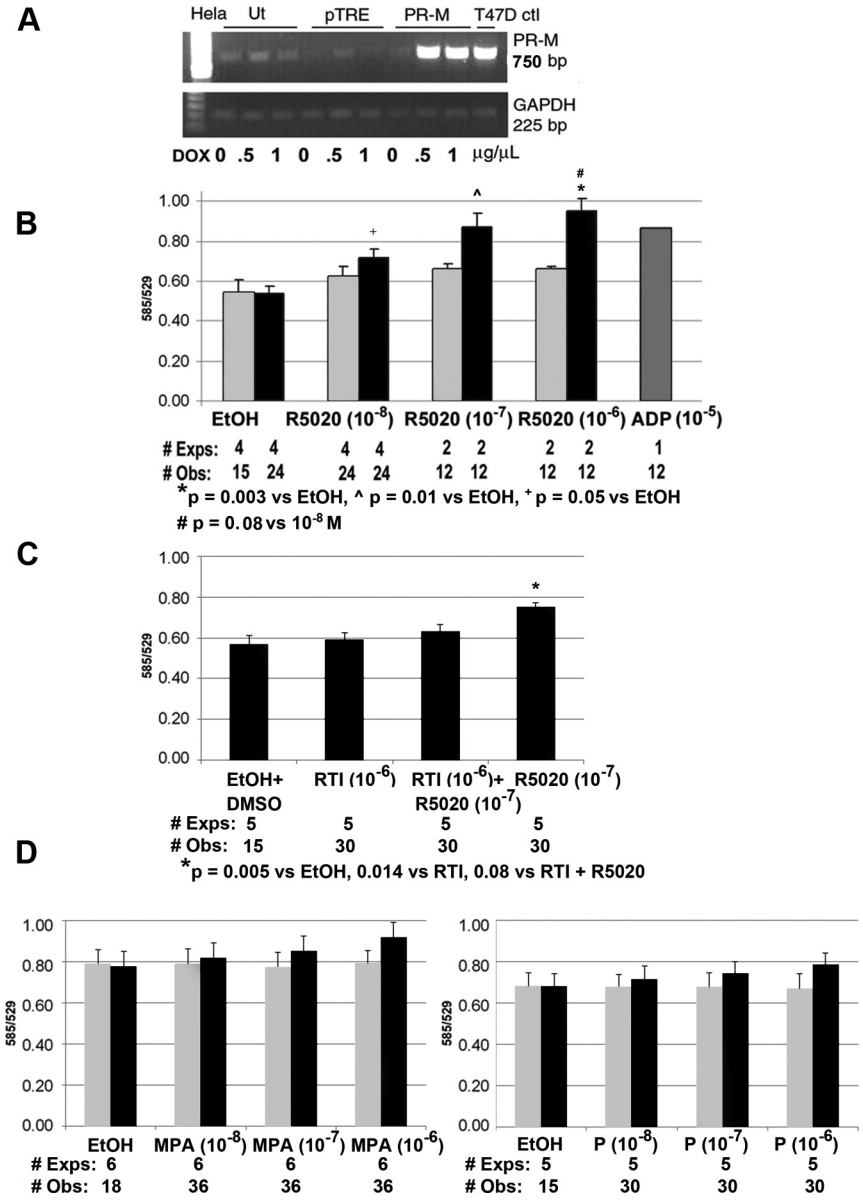

Figure 6. Change in mitochondrial activity in Tet-On HeLa cells expressing PR-M. A, Ethidium bromide-stained gel of RT-PCR product for *PR-M* in Tet-On HeLa cells after doxycycline (DOX) induction (Ut, untransfected; pTRE, control plasmid; PR-M, pTRE plasmid with PR-M cDNA). B, An increase in ψm in Tet-On HeLa cells expressing PR-M (dark bars) was seen after 30 minutes treatment with R5020. No significant change in ψm was seen in control transfected cells (light bars). Treatment with ADP (10^{-5}M) served as a positive control. C, The increase in ψm in Tet-On HeLa cells expressing PR-M seen after 30 minutes treatment with R5020 was inhibited by cotreatment with the PR antagonist RTI-6413-049b. D, No significant change was seen in ψm with MPA (left) or progesterone (right) treatment for 60 minutes in Tet-On HeLa cells expressing PR-M (dark bars) or control transfected cells (light bars). A positive linear trend was seen in the percent difference of MPA to ethanol (F = 5.17, P = .038) and in the percent difference of P to ethanol (F = 4.76, P = .05). In control transfected Tet-on HeLa cells, there was no linear trend in the percent difference of MPA to ethanol (F = 0.059, P = .811) or in the percent difference of progesterone to ethanol (F = 0.3, P = .59) (Supplemental Figure 7). All values are expressed as mean ± SEM. Abbreviations: DMSO, dimethylsulfoxide; EtOH, ethanol; #Exps, number of experiments performed on different days; #Obs, total number of wells assayed; P, progesterone.

chondrial proteins in which the remainder of the protein extends into the cytosol. In studies with the mitochondrial protein Tom 70, at least 3 basic amino acids on the C-terminal flanking region of the transmembrane domain were necessary for mitochondrial localization (33).

The structure of PR-M and the lack of specific antibodies make protein determination difficult. Compared with nPR, the only unique sequence is comprised of 16 N-terminal amino acids proposed to be part of the MLS. The high hydrophobicity and poor antigenicity of this sequence preclude synthesis of a specific antibody. Additionally, the specificity of commercial antibodies to the HBD of nPR has been questioned (26) given the multiple bands visible on Western blot analyses, compared with fewer bands seen with antibodies directed to the N terminus. These multiple bands have been attributed to nonspecific binding and/or proteolytic fragments. For these reasons, we verified the specificity of the 2 antibodies (C19 and MAB 462) in recognizing PR-M with expression of a recombinant protein and identification of endogenous PR-M by mass spectrometry. For the latter, mitochondria were isolated from freshly collected human myometrium followed by a protein isolation optimized for membrane proteins using Triton X-114 detergent (14). This was followed by an immunoprecipitation with the MAB 462 antibody. Mass spectrometry identified a PR peptide encoded by the last 2 exons of PR-M in an excised band at 38 kDa. It is not possible to totally exclude this peptide originating from a proteolytic fragment of nPR. But we consider this very unlikely given the stringency of the technique and that no other nuclear proteins were identified in the band. Identified proteins included mitochondrial inner membrane protein (IMMT), mitochondrial aconitate hydratase (ACON), and myosin heavy chain (Myh11), which is known to be identified in muscle mitochondrial preparations (34). Ig κ-chain C (IGKC) was thought to be a contaminant from the immunoprecipitation.

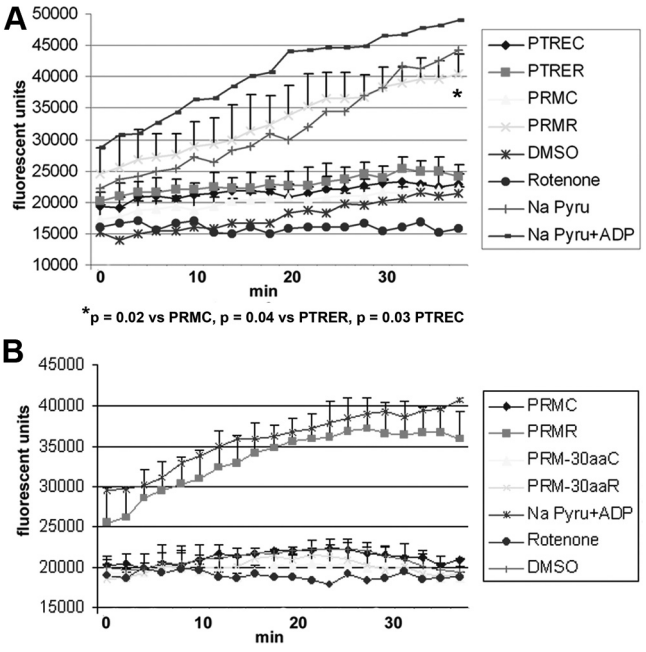

Figure 7. Change in extracellular oxygen levels in Tet-On HeLa cells expressing PR-M. A, A decrease in extracellular oxygen levels (reflected by an increase in probe emission) was seen in Tet-On HeLa cells expressing PR-M treated with 10^{-8}M R5020 (PRMR). Using repeated-measures analysis adjusting for time effect, PRMR was significantly different from cells expressing PR-M treated with vehicle (PRMC), control transfected cells treated with R5020 (PTRER), and control transfected cells treated with vehicle (PTREC). Results are from duplicate experiments (mean ± SD). B, Tet-On HeLa cells expressing a truncated form of PR-M lacking the initial 30 amino acids (PR-M-30aa) showed no evidence of a change in oxygen levels with 10^{-8}M R5020 (PR-M-30aaR) treatment or vehicle (PR-M-30aaC) in duplicate experiments (mean ± SD). Positive controls included treatment of pTRE transfected cells with sodium pyruvate (Pyru) (4mM) plus ADP (10^{-5}M) or sodium pyruvate (4mM) alone, whereas negative controls included treatments with rotenone (10μM) or dimethylsulfoxide (DMSO).

PR-M represents the first steroid receptor localized to the mitochondrion with a putative MLS. Localization of a fraction of nuclear steroid and thyroid receptors to mitochondria has been previously reported including the glucocorticoid receptor (GRα) (35), estrogen receptor (ERα and ERβ) (36, 37) and thyroid receptor (38). The function of these receptors is proposed to be regulation of mitochondrial gene transcription (39, 40).

The lack of a DBD in PR-M precludes regulation of gene transcription. Appropriate ligand binding to PR-M is supported by the identical HBD of the nPR and by a previous study showing that a construct of the hinge plus HBD, which would be equivalent to PR-M without the unique N terminus, has the same ligand-binding characteristics as the native nPR (41).

Our studies of silencing and overexpression of PR-M show a role for the receptor in the control of mitochondrial activity. The progestin R5020 induced an increase in ψm with a corresponding increase in cellular oxygen consumption, consistent with increased cellular respiration. The use of JC-1 as a ψm indicator has been both supported (42, 43) and criticized (44, 45). JC-1 is a cationic membrane-permeant compound that distributes within the cell according to electrical charge. In the cytoplasm, JC-1 is a monomer with primary emission in the green fluorescent range. In the mitochondrial matrix, low potential causes dye stacking (JC-1 aggregates) resulting in a shift to red fluorescent emission. The ratio of red to green emission shows a direct correlation with ψm. This assumption has been questioned due to several observations. Confocal microscopy has shown heterogeneous mitochondrial staining within the same cell, not seen with other types of fluorescent dyes (46). The change in red fluorescence appears to be more sensitive than the change in green fluorescence ψm (47). Changes in plasma membrane potential without a change in the ψm may lead to changes in the emission ratio (45). Because of these concerns, we corroborated our finding of increased ψm with a different fluorometric dye, TMRM. TMRM, another cationic membrane-permeant dye, distributes within the cell based on electrical potential and shows a linear fluorescent emission with concentration, when used at a low concentration of 10nM to 30nM (45). The ψm assays performed in this study were not kinetic; thus, the energy status of the cells with different treatments were being compared at a given time point. In a kinetic assay, an increase in ATP production is associated with a temporary decrease in ψm as the proton extrusion increases (49). This quickly returns to a new steady state in the condition of substrate availability. Our results show a more energized cell after progestin treatment via PR-M with corresponding increased oxygen consumption consistent with increased cellular respiration. This is under conditions of substrate excess. If substrate was not available, the proton gradient would be depleted, leading to depolarization. Examples of other cells showing an increase in ψm with increased cellular respiration are found. Treatment of cultured hepatocytes with vasopressin results in a calcium-dependent increase in nicotinamide adenine dinucleotide phosphate, increased ψm, and a corresponding increase in cellular respiration (50–52).

An increase in ψm was seen with progesterone, MPA, and R5020. The latter was used for most of the experiments due to increased potency and receptor specificity. R5020 has little or no reaction with the GR. Using a glucocorticoid response element transfection assay in 1470.2 cells (a mouse mammary carcinoma cell line), no activation of endogenous GR was seen at a dose of 30nM R5020 (53). Likewise, treatment with a specific PR antagonist, RTI-6413-049b, blocked the increase in ψm seen with R5020. Unlike RU-486, RTI 6413-049b lacks

any PR agonist effects; lacks binding of ERα, ERβ, and androgen receptor; and has much less of an antiglucocorticoid effect (54).

Physiological observations support a role for progesterone in increasing mitochondrial activity. Approximately 68% of the basal metabolic rate (MR) is due to mitochondrial ATP production (55). The MR varies during the menstrual cycle and with pregnancy, consistent with a role for progesterone. In women, resting MR increases 8.8% during the progesterone-dominant luteal phase (56, 57). Female athletes with short luteal phases and decreased progesterone levels have a lower resting MR compared with athletes of similar body mass index with normal luteal phases. This is not explained by differences in thyroid function, food intake, or fat mass (58). Resting MR increases 39% during pregnancy, with the greatest increase in the second and third trimesters (59). Taken together, these patterns correlate with circulating progesterone levels.

On an organ level, the heart requires a dramatic increase in energy production for pregnancy. Pregnancy results in an approximate 49% increase in cardiac output, 32% increase in heart rate, and 15% increase in stroke volume (60). Given the large number of mitochondria in the ventricle, progesterone action via PR-M may play a major role in stimulating cardiac energy production.

Since our report of cloning PR-M in 2003 (9), one other paper has detailed investigation of this protein. In 2008, Samalecos and Gellerson (26) identified transcript for *PR-M* by conventional RT-PCR followed by Southern blot analysis in T47D breast cancer cells and myometrial cells. They were unable to identify the endogenous protein with Western blot analysis or express the protein in a rabbit lysate reticulocyte system. We believe that lack of identification of endogenous protein may be due to low abundance. The investigators used whole-cell protein preparations, typically with 30 μg protein for Western blot analysis. Our experiments with whole-cell protein preparations used 80 to 120 μg total protein for Western blot analysis. Purified mitochondrial protein preparations required much lower amounts of protein. The TNT T7 Quick Coupled Transcription/Translation system (Promega Corp, Madison, Wisconsin) used by these investigators is designed for soluble proteins. Typically, the addition of canine pancreatic microsomes is required for membrane protein expression (48). In our experiments, in vitro transcription/translation was performed with a cell-free *E. coli* system. We found the addition of Triton X-100 detergent necessary for expression. Additionally, purification was enhanced by use of a HIS-tag and nickel column.

We acknowledge that the evidence for PR-M is mostly correlative and does not unequivocally prove the existence of this protein. This is due to the unique structure of PR-M that precludes specific antibody production. Because of this, we have used many techniques to support the presence of PR-M, including verification of a PR peptide by mass spectrometry at the expected mass of PR-M in a mitochondrial protein preparation, identification of a protein at the expected mass of PR-M with Western blot analysis using cells proven to lack expression of nPR, use of selective antibodies that should and should not recognize PR-M, and functional assays with either silencing or overexpression of PR-M showing a biological effect.

In conclusion, our molecular approaches suggest that PR-M is the first steroid receptor that expresses a putative MLS correctly situated on one end of the protein and is localized primarily to the mitochondrion. Our functional studies indicate that progesterone directly affects mitochondrial activity via this novel receptor. A progesterone-dependent increase in cellular respiration may play a role in many physiological processes ranging from modulation of cellular respiration in the developing embryo to a more global impact on tissues requiring increased energy to meet the metabolic demands of pregnancy.

Acknowledgments

We thank Donald McDonnell, PhD, for the kind gift of RTI-6413-049b and technical assistance and Dr Katherine Horwitz for the gift of T47D-Y cells. We thank Richard Auten, MD, for technical assistance with mitochondrial membrane potential assays. We thank Laura Dubois and J. Will Thompson, PhD, of the Duke University Proteomics Core Facility for mass spectrometry analysis. The Research-on-Research Group of Duke University assisted with statistical analysis. Technical assistance was provided by the Duke University Sequencing Facility and the Duke University Microscopy Service.

Address all correspondence and requests for reprints to: Thomas M. Price, MD, Division of Reproductive Endocrinology, Duke University Medical Center, 5704 Fayetteville Road, Durham, North Carolina 27713. E-mail: price067@mc.duke.edu.

This work was supported by the American Heart Association (Mid-Atlantic Affiliate), NIH/NIHCD 1R03HD052770-01, a Department of Defense Breast Cancer Idea Award, the Charles Hammond Foundation of Duke University, and the Susan Fiery-Hughes Foundation of Duke University.

Disclosure Summary: The authors have nothing to disclose.

References

1. **Wen DX, Xu YF, Mais DE, Goldman ME, McDonell DP.** The A and B isoforms of the human progesterone receptor operate through

distinct signaling pathways within target cells. *Mol Cell Biol*. 1994; 14:8356–8364.
2. **Jacobsen BM, Richer JK, Sartorius CA, Horwitz KB.** Expression profiling of human breast cancers and gene regulation by progesterone receptors. *J Mammary Gland Biol Neoplasia*. 2003;8:257–268.
3. **Tian J, Kim S, Heilig E, Ruderman J.** Identification of XPR-1, a progesterone receptor required for *Xenopus* oocyte activation. *Proc Natl Acad Sci U S A*. 2000;97:14358–14363.
4. **Zhu Y, Rice CD, Pang Y, Pace M, Thomas P.** Cloning, expression, and characterization of a membrane progestin receptor and evidence it is an intermediary in meiotic maturation of fish oocytes. *Proc Natl Acad Sci U S A*. 2003;100:2231–2236.
5. **Meyer C, Schmid R, Scriba PC, Wehling M.** Purification and partial sequencing of high-affinity progesterone-binding site(s) from porcine liver membranes. *Eur J Biochem*. 1996;239:726–731.
6. **Gerdes D, Wehling M, Leube B, Falkenstein E.** Cloning and tissue expression of two putative steroid membrane receptors. *Biol Chem*. 1998;379:907–911.
7. **Boonyaratanakornkit V, Scott MP, Ribon V, et al.** Progesterone receptor contains a proline-rich motif that directly interacts with SH3 domains and activates c-Src family tyrosine kinases. *Mol Cell*. 2001;8:269–280.
8. **Boonyaratanakornkit V, McGowan E, Sherman L, Mancini MA, Cheskis BJ, Edwards DP.** The role of extranuclear signaling actions of progesterone receptor in mediating progesterone regulation of gene expression and the cell cycle. *Mol Endocrinol*. 2007;21:359–375.
9. **Saner KJ, Welter BH, Zhang F, et al.** Cloning and expression of a novel, truncated progesterone receptor. *Mol Cell Endocrinol*. 2003; 200:155–163.
10. **Sartorius CA, Groshong SD, Miller LA, et al.** New T47D breast cancer cell lines for the independent study of progesterone B- and A-receptors: only antiprogestin-occupied B-receptors are switched to transcriptional agonists by cAMP. *Cancer Res*. 1994;54:3868–3877.
11. **Price TM, Hansen EL, Oliver TN.** Immunofluorescent localization of a novel progesterone receptor(s) in a T47D-Y breast cancer cell line lacking genomic progesterone receptor expression. *J Soc Gynecol Investig*. 2005;12:610–616.
12. **Wilm M, Shevchenko A, Houthaeve T, et al.** Femtomole sequencing of proteins from polyacrylamide gels by nano-electrospray mass spectrometry. *Nature*. 1996;379:466–469.
13. **Scholte HR, Yu Y, Ross JD, Oosterkamp II, Boonman AM, Busch HF.** Rapid isolation of muscle and heart mitochondria, the lability of oxidation phosphorylation and attempts to stabilize the process *in vitro* by taurine, carnitine and other compounds. *Mol Cell Biochem*. 1997;174:61–66.
14. **Everberg H, Sivars U, Emanuelsson C, et al.** Protein pre-fractionation in detergent-polymer aqueous two-phase systems for facilitated proteomic studies of membrane proteins. *J Chromatogr A*. 2004;1029:113–124.
15. **Greenawalt J.** The isolation of outer and inner mitochondrial membranes. *Methods Enzymol*. 1974;31:310–323.
16. **Behera MA, Dai Q, Garde R, Saner C, Jungheim E, Price TM.** Progesterone stimulates mitochondrial activity with subsequent inhibition of apoptosis in MCF-10A benign breast epithelial cells. *Am J Physiol Endocrinol Metab*. 2009;297:E1089–E1096.
17. **Huang S.** Development of a high throughput screening assay for mitochondrial membrane potential in living cells. *J Biomol Screen*. 2002;7:383–389.
18. **Livak KJ, Schmittgen TD.** Analysis of relative gene expression data using real-time quantitative PCR and the $2^{-\Delta\Delta C_T}$ method. *Methods*. 2001;25:402–408.
19. **Guiochon-Mantel A, Loosfelt H, Lescop P, et al.** Mechanisms of nuclear localization of the progesterone receptor: evidence for interaction between monomers. *Cell*. 1989;57:1147–1154.
20. **Wei LL, Krett NL, Francis MD, et al.** Multiple progesterone receptor ribonucleic acids and their autoregulation by progestin agonists and antagonists in breast cancer cells. *Mol Endocrinol*. 1988;2:62–72.
21. **Wei L, Miner R.** Evidence for the existence of a third progesterone receptor protein in human breast cancer cell line T47D. *Cancer Res*. 1994;54:340–343.
22. **Moran TJ, Gray S, Mikosz CA, Conzen SD.** The glucocorticoid receptor mediates a survival signal in human mammary epithelial cells. *Cancer Res*. 2000;60:867–872.
23. **Coppock HA, Gilham DE, Howell A, Clarke RB.** Cyclin-dependent kinase inhibitors and basement membrane interact to regulate breast epithelial cell differentiation and acinar morphogenesis. *Cell Prolif*. 2007;40:721–740.
24. **Nardulli AM, Katzenellenbogen BS.** Progesterone receptor regulation in T47D human breast cancer cells: analysis by density labeling of progesterone receptor synthesis and degradation and their modulation by progestin. *Endocrinology*. 1988;122:1532–1540.
25. **Cho H, Aronica SM, Katzenellenbogen BS.** Regulation of progesterone receptor gene expression in MCF-7 breast cancer cells: a comparison of the effects of cyclic adenosine 3′,5′-monophosphate, estradiol, insulin-like growth factor-I, and serum factors. *Endocrinology*. 1994;134:658–664.
26. **Samalecos A, Gellersen B.** Systematic expression analysis and antibody screening do not support the existence of naturally occurring progesterone receptor (PR)-C, PR-M, or other truncated PR isoforms. *Endocrinology*. 2008;149:5872–5887.
27. **Wan Y, Coxe KK, Thackray VG, Housley PR, Nordeen SK.** Separable features of the ligand-binding domain determine the differential subcellular localization and ligand-binding specificity of glucocorticoid receptor and progesterone receptor. *Mol Endocrinol*. 2001;15:17–31.
28. **Hanson BJ, Schulenberg B, Patton WF, Capaldi RA.** A novel subfractionation approach for mitochondrial proteins: a three-dimensional mitochondrial proteome map. *Electrophoresis*. 2001;22: 950–959.
29. **Richer JK, Jacobsen BM, Manning NG, Abel MG, Wolf DM, Horwitz KB.** Differential gene regulation by the two progesterone receptor isoforms in human breast cancer cells. *J Biol Chem*. 2002; 277:5209–5218.
30. **Burnstock G.** Purine and pyrimidine receptors. *Cell Mol Life Sci*. 2007;64:1471–1483.
31. **Mac Namara P, Loughrey HC.** Progesterone receptor A and B isoform expression in human osteoblasts. *Calcif Tissue Int*. 1998;63: 39–46.
32. **Bannai H, Tamada Y, Maruyama O, Nakai K, Miyano S.** Extensive feature detection of N-terminal protein sorting signals. *Bioinformatics*. 2002;18:298–305.
33. **Rapaport D.** Finding the right organelle. Targeting signals in mitochondrial outer-membrane proteins. *EMBO Rep*. 2003;4:948–952.
34. **Taylor SW, Fahy E, Zhang B, et al.** Characterization of the human heart mitochondrial proteome. *Nat Biotechnol*. 2003;21:281–286.
35. **Psarra AM, Solakidi S, Trougakos IP, Margaritis LH, Spyrou G, Sekeris CE.** Glucocorticoid receptor isoforms in human hepatocarcinoma HepG2 and SaOS-2 osteosarcoma cells: presence of glucocorticoid receptor α in mitochondria and of glucocorticoid receptor β in nucleoli. *Int J Biochem Cell Biol*. 2005;37:2544–2558.
36. **Chen JQ, Delannoy M, Cooke C, Yager JD.** Mitochondrial localization of ERα and ERβ in human MCF7 cells. *Am J Physiol Endocrinol Metab*. 2004;286:E1011–E1022.
37. **Yang S, Liu R, Perez E, et al.** Mitochondrial localization of estrogen receptor β. *Proc Natl Acad Sci U S A*. 2004;101:4130–4135.
38. **Scheller K, Seibel P, Sekeris C.** Glucocorticoid and thyroid hormone receptors in mitochondria of animal cells. *Int Rev Cytol*. 2003;222: 1–61.
39. **Tsiriyotis C, Spandidos DA, Sekeris CE.** The mitochondrion as a

primary site of action of glucocorticoids: mitochondrial nucleotide sequences, showing similarity to hormone response elements, confer dexamethasone inducibility to chimaeric genes transfected in LATK$^-$ cells. *Biochem Biophys Res Commun*. 1997;235:349–354.
40. **Psarra AM, Solakidi S, Sekeris CE.** The mitochondrion as a primary site of action of steroid and thyroid hormones: presence and action of steroid and thyroid hormone receptors in mitochondria of animal cells. *Mol Cell Endocrinol*. 2006;246:21–33.
41. **Tetel MJ, Jung S, Carbajo P, Ladtkow T, Skafar DF, Edwards DP.** Hinge and amino-terminal sequences contribute to solution dimerization of human progesterone receptor. *Mol Endocrinol*. 1997;11:1114–1128.
42. **Cossarizza A, Ceccarelli D, Masini A.** Functional heterogeneity of an isolated mitochondrial population revealed by cytofluorometric analysis at the single organelle level. *Exp Cell Res*. 1996;222:84–94.
43. **Mathur A, Hong Y, Kemp BK, Barrientos AA, Erusalimsky JD.** Evaluation of fluorescent dyes for the detection of mitochondrial membrane potential changes in cultured cardiomyocytes. *Cardiovascular Research*. 2000;46:126–138.
44. **Bernardi P, Scorrano L, Colonna R, Petronilli V, Di Lisa F.** Mitochondria and cell death. Mechanistic aspects and methodological issues. *Eur J Biochem*. 1999;264:687–701.
45. **Duchen MR, Surin A, Jacobson J.** Imaging mitochondrial function in intact cells. *Methods Enzymol*. 2003;361:353–389.
46. **Smiley ST, Reers M, Mottola-Hartshorn C, et al.** Intracellular heterogeneity in mitochondrial membrane potentials revealed by a J-aggregate-forming lipophilic cation JC-1. *Proc Natl Acad Sci U S A*. 1991;88:3671–3675.
47. **Di Lisa F, Blank PS, Colonna R, et al.** Mitochondrial membrane potential in single living adult rat cardiac myocytes exposed to anoxia or metabolic inhibition. *J Physiol*. 1995;486:1–13.
48. **Falk MM, Buehler LK, Kumar NM, Gilula NB.** Cell-free synthesis and assembly of connexins into functional gap junction membrane channels. *EMBO J*. 1997;16:2703–2716.
49. **Nicholls DG, Ward MW.** Mitochondrial membrane potential and neuronal glutamate excitotoxicity: mortality and millivolts. *Trends Neurosci*. 2000;23:166–174.
50. **Robb-Gaspers LD, Burnett P, Rutter GA, Denton RM, Rizzuto R, Thomas AP.** Integrating cytosolic calcium signals into mitochondrial metabolic responses. *EMBO J*. 1998;17:4987–5000.
51. **Duchen M.** Mitochondria and calcium: from cell signalling to cell death. *J Physiol*. 2000;529(Pt 1):1:57–68.
52. **Rizzuto R, Bernardi P, Pozzan T.** Mitochondria as all-round players of the calcium game. *J Physiol*. 2000;529(Pt 1):1:37–47.
53. **Giannoukos G, Szapary D, Smith CL, Meeker JE, Simons SS Jr.** New antiprogestins with partial agonist activity: potential selective progesterone receptor modulators (SPRMs) and probes for receptor- and coregulator-induced changes in progesterone receptor induction properties. *Mol Endocrinol*. 2001;15:255–270.
54. **Sathya G, Jansen MS, Nagel SC, Cook CE, McDonnell DP.** Identification and characterization of novel estrogen receptor-β-sparing antiprogestins. *Endocrinology*. 2002;143:3071–3082.
55. **Hulbert AJ, Else PL.** Mechanisms underlying the cost of living in animals. *Annu Rev Physiol*. 2000;62:207–235.
56. **Buffenstein R, Poppitt SD, McDevitt RM, Prentice AM.** Food intake and the menstrual cycle: a retrospective analysis, with implications for appetite research. *Physiol Behav*. 1995;58:1067–1077.
57. **Webb P.** 24-hour energy expenditure and the menstrual cycle. *Am J Clin Nutr*. 1986;44:614–619.
58. **Lebenstedt M, Platte P, Pirke KM.** Reduced resting metabolic rate in athletes with menstrual disorders. *Med Sci Sports Exerc*. 1999;31:1250–1256.
59. **Koop-Hoolihan LE, van Loan MD, Wong WW, King JC.** Longitudinal assessment of energy balance in well-nourished, pregnant women. *Am J Clin Nutr*. 1999;69:697–704.
60. **Hennessy TG, MacDonald D, Hennessy MS, et al.** Serial changes in cardiac output during normal pregnancy: a Doppler ultrasound study. *Eur J Obstet Gynecol Reprod Biol*. 1996;70:117–122.